

Genome-wide association mapping of genotype-environment interactions affecting yield-related traits of spring wheat grown in three watering regimes

Alaa A. Said^a, Alice H. MacQueen^b, Haitham Shawky^c, Matthew Reynolds^d, Thomas E. Juenger^b, Mohamed El-Soda^{e,*},¹

^a Department of Agronomy, Faculty of Agriculture, Sohag University, Sohag, Egypt

^b Department of Integrative Biology, University of Texas at Austin, Austin, TX, USA

^c Department of Microbiology, National Research Centre, Egypt

^d International Maize and Wheat Improvement Center (CIMMYT), Carretera Mexico, El Batan, Texcoco, Mexico

^e Department of Genetics, Faculty of Agriculture, Cairo University, Giza 12613, Egypt

ARTICLE INFO

Keywords:

Association mapping
Canopy temperature
Chlorophyll content
Drought
Genotype-environment interaction
Grain yield
Spring bread wheat
Yield components

ABSTRACT

Genotype-environment interaction (GxE) has a great impact on wheat physiology, morphology and grain yield (GY). We evaluated an association mapping panel of spring wheat advanced lines for chlorophyll content, canopy temperature (CT), and yield-related traits under three different watering regimes in two consecutive growing seasons. Genome-wide association mapping identified 457 SNPs, with significant effects that varied with the watering regimes and growing seasons, of which 199 and 69 SNPs showed pleiotropic and conditionally neutral effects, respectively, on the measured traits. We mapped 61 SNPs with effects higher than 10% on all traits, showing antagonistic pleiotropic effects on CT, corresponding to 46 genes; some of these genes represent good candidates to control wheat response to water availability. Surprisingly, no significant SNPs were mapped in the semi-dwarfing genes, *Rht-B1b* or *Rht-D1b*. However, haplotype analysis of the SNPs located at the positions of both genes revealed significant interactions of GY with the watering regimes for *Rht-B1b* and with the growing season for *Rht-D1b*. We selected genotypes that outperformed two local check cultivars; some of them overlapped across the three watering regimes and could be used to create a multi-parent population to further unravel the genetic factors underlying yield component traits across drought stress. Our results demonstrate the importance of incorporating GxE in mapping models to better understand wheat response to different watering regimes and to select stable markers for selection.

1. Introduction

Wheat (*Triticum aestivum* L.) is one of the world's most important crops with a global production of 761.5 million tons (FAOSTAT 2019). It has been predicted that wheat production would need to reach 858 million tons by 2050 in order to meet the predicted global food demand caused by the increase in the world population (Alexandratos and Bruinsma, 2012). However, wheat production and productivity are threatened by biotic and abiotic stresses. Drought is the most significant of these stresses and is being exacerbated by climate change (Edae et al., 2014; Shahinnia et al., 2016; Mathew et al., 2019; Reynolds et al., 2021). Therefore, breeding drought-tolerant wheat genotypes with

relevant agronomic and adaptive traits by discovering the underlying genes and alleles is critical for increasing grain yield (GY) (Shahinnia et al., 2016).

Drought-tolerant and agronomically superior wheat lines are continuously being developed for evaluation and use in breeding programs by the International Maize and Wheat Improvement Center (CIMMYT) and other national and international breeding programs (Manès et al., 2012; Reynolds et al., 2021). Several studies have genetically dissected wheat yield and its components such as plant height (PH), spike length (SPKL), number of spikes (SPKN), and number of tillers (TN), in response to drought stress (Edae et al., 2014; Mwadzingeni et al., 2016). Yield-component traits and biological yield (BY),

* Corresponding author.

E-mail address: mohamed.elsoda@agr.cu.edu.eg (M. El-Soda).

¹ <https://orcid.org/0000-0002-6930-5246>.

whole plant dry biomass, are positively correlated traits with GY under water limiting conditions (Chen et al., 2012; Mwadzingeni et al., 2016). Chlorophyll content (Chl) has been found to be positively correlated with GY, (Pinto et al., 2010; Sid'ko et al., 2017), while canopy temperature (CT), measured at the vegetative and grain filling stages, was negatively correlated with GY (Pinto et al., 2010; Lopes et al., 2013).

In general, the expression of any morphological or physiological trait is influenced by the underlying genetic make-up (G), the surrounding environment (E), and their interactions (GxE). Yield and its related traits are quantitative and polygenic, or complex traits. They are continuously distributed, controlled by quantitative trait loci (QTL), genomic regions that contain the associated genes, and heavily influenced by the environment. As a result, QTL or genes affecting physiological traits, yield and its components are environmentally sensitive, or have different effects in different environments and therefore exhibit QTL-environment interaction (QTLxE). For example, QTL can have synergistic pleiotropic effects, i.e. a QTL with positive effects on two or more traits, or antagonistic pleiotropic effects, i.e., a QTL with opposite effects on two or more traits. In addition, they can show conditionally neutral effects, i.e. a QTL with a significant effect on a trait in one environment, but no effects in other environments. The overall pattern of QTL x E effects can constrain or facilitate responses to artificial selection (Falconer, 1952). Therefore, these effects are critical and should be carefully addressed in breeding programs (Des Marais et al., 2013; El-Soda et al., 2014).

Two approaches can be used to map QTL and to identify genes with underlying natural variation affecting phenotypes: traditional QTL mapping, and genome-wide association mapping (GWAM). Traditional QTL mapping approach relies on using the offspring of structured crosses, such as recombinant inbred lines (RIL), backcrosses (BC), and doubled haploids (DH). GWAM uses panels of genotypes collected from naturally evolved and adapted populations, or breeding lines, and can often identify smaller QTL intervals by making elegant use of the historical recombination events that have occurred over thousands of generations. To obtain fine-mapping resolution, it is critical to use a large number of diverse and densely genotyped accessions in GWAM studies. In high recombination regions of the genome, this can narrow the associated region to one or a few genes, eliminating the need for further fine-mapping (Alqudah et al., 2020; El-Soda and Sarhan, 2021). These associations and candidate genes may provide key markers for trait introgression, marker-assisted selection, or targets for functional manipulation for crop improvement.

The total wheat production in Egypt does not meet the current demand, and due to the limited area available for agricultural use, there is a need to expand wheat production into newly reclaimed areas that suffer from abiotic stresses such as drought. Here, we map the genetic factors underlying Chl, CT, PH, TN, SPKL, SPKN, BY, GY, and harvest index (HI) and their interaction with water availability in order to select genotypes that outperform local, drought-tolerant, and high-yielding check cultivars.

2. Materials and methods

2.1. Plant material and experimental setup

We used the wheat association mapping initiative (WAMI) population (Lopes et al., 2015), a set of 287 diverse advanced wheat lines, genotyped with 26814 SNPs (Ahirwar et al., 2018) and released by the International Maize and Wheat Improvement Center (CIMMYT). In addition, two local Egyptian check cultivars were used: Sahel-1, a drought-tolerant cultivar, and Shandweel-1, a local commercial cultivar adapted to the Sohag governorate. All plant materials were evaluated in two field experiments during the two consecutive growing seasons 2017/2018 (17/18) and 2018/2019 (18/19) at the Experimental Farm of Faculty of Agriculture, Sohag University, Egypt. Both experiments were sown in November and harvested in April. As a newly reclaimed soil, the texture of soil was sandy clay loam, from 0 to 30 cm, followed

by sandy loam soil, from 30 to 45 cm at the experimental farm. The experimental design was a complete randomized block design in a strip plot arrangement with three replicates per watering regime. Each irrigation strip was surrounded by a dry strip of 3 m width and two dry canals of 50 cm depth to maintain the desired watering level and prevent groundwater from flowing between treatments. Watering regimes were arranged horizontally and genotypes were arranged vertically. All genotypes were represented in each experimental block and each genotype was grown in two rows, spaced 20 cm apart. Each row was two meters in length with a space of 10 cm between plants within each row. Each experiment received 238 kg ha⁻¹ ammonium nitrate (33.5% N), 75 kg ha⁻¹ calcium superphosphate (15.5% P₂O) and 58 kg ha⁻¹ potassium sulfate (48% K₂O).

The two physiological traits, Chl and CT, were measured on the flag leaf after the anthesis stage, using a SPAD-502 chlorophyll meter (Minolta, Japan) and infrared thermometer, Model 8866, JQA Instrument, Inc. (Tokyo, Japan), respectively. Yield component traits were measured at harvest. For each replicate, 10 plants were randomly chosen for phenotypic evaluation. PH was measured in centimeters (cm) from the ground to the tip of the spike. In addition, TN, SPKL, SPKN, BY, GY and HI were measured at maturity for each plant.

2.2. Watering treatments

The amount of evapotranspiration (ETp) during each watering cycle was calculated for a soil depth of 45 cm as the difference between soil moisture contents after watering and before the next watering. For an area of 4200.8 m² (one feddan = 0.42 hectare), ETp in m³ can be calculated using the following equation:

$$ETp = (\theta_2 - \theta_1) / 100 \times Bd \times (D/100) \times 4200.8$$

Where θ_2 is the percent of soil moisture after irrigation, θ_1 is the percent of soil moisture before the next irrigation, D is the soil depth, and Bd is the bulk density of the soil (g/cm³).

Soil samples were collected at three depths directly before watering and 48 h after. The amount of water (Q), in m³, for each watering treatment was computed according to the following formula:

$$Q = R \times D \times Bd \times (F.C. - S.M.I.) / 100$$

Where Q is the amount of water, R is the area to be watered, D is the soil depth to be watered, Bd is the bulk density of the soil (gm/cm³), F.C is the field capacity in percent, and S.M.I. is the percentage of soil moisture before irrigation.

A water meter was used to measure the amount of water, in cm³, needed to raise the soil moisture of the upper 45 cm layer to the field capacity (FC). Water applied to the plots at each watering treatment was equal to the difference between the soil moisture at the FC and at irrigation time plus 10% of water to ensure a good uniform distribution of water through the plots (Table 1). As reported earlier (Allen et al., 1998), the three watering treatments used here were; well-watered = 0.8 of the ETp, mild drought stress = 0.6 of the ETp, and severe drought stress = 0.4 of the ETp.

2.3. Statistical analysis

The raw data of each experiment was used for statistical analysis using SPSS v21. Analysis of variance (ANOVA) was used to test for significant differences between genotypes (G), irrigation treatments (T), and their interaction (G × T). Broad-sense heritability (H²) was estimated for each trait as the ratio between the genetic variance (δ^2g) and the total phenotypic variance (δ^2ph) as follows;

$$H^2 = \delta^2g / \delta^2ph$$

$$\delta^2ph = \delta^2g + \delta^2e$$

Table 1

Seasonal evapotranspiration, seasonal irrigation requirements, and number of irrigation for the three treatments in the two seasons (17/18 and 18/19).

Treatments	Seasonal evapotranspiration (mm)			Seasonal irrigation requirement (m ³ /fed)			Number of irrigations	
	17/18	18/19	mean	17/18	18/19	mean	17/18	18/19
Well-watered	523.1	580.7	551.9	1675.6	1867.2	1771.4	11	12
Mild stress	391.8	435.6	413.7	1194.4	1385.1	1289.8	8	9
Severe stress	260.5	290.4	275.5	970.5	1081.4	1026.0	5	6

$$\delta^2 g = (MS_g - MS_e) / r$$

$$\delta^2 e = MS_e$$

Where $\delta^2 e$ is the error variance, MS_g is the mean square of genotypes, MS_e is the error mean square, and r is the number of replications. Genotype means were compared using the Revised Least Significant Differences test (RLSD).

2.4. Genome-wide association mapping

We analyzed SNP effects determined using univariate GWAS on phenotypes using multivariate adaptive shrinkage (mash) analysis (Urbut et al., 2019) to find genomic associations with significant effects on one or more phenotypes. For the majority of genotypes, one phenotypic measurement was taken for three replicates for each treatment and year. Outlier phenotypic values were removed before analysis for Chl and CT. Using the remaining data, BLUPs for each combination of phenotype, treatment, and year were calculated in the rrBLUP package in R, using a kinship matrix. The kinship matrix was calculated using default methods in GAPIT. Univariate GWAS analyses were performed using the 'big_univLinReg' function in bigsnpr using principal components for population structure correction computed using the 'snr_autoSVD' function (Privé et al., 2018, 2020; MacQueen et al., 2021). The optimum number of principal components (PCs) to account for population structure was determined using model selection, by selecting the number of PCs that caused the genomic inflation factor (λ_{GC}) to be closest to 1 (Supplementary Table 1). To test the significance of SNP effect estimates in many conditions (for example, across multiple years and phenotypes) we used mash, a flexible, data-driven method that shares information on patterns of effect size and sign in any dataset where effects can be estimated on univariate conditions for many conditions and SNPs (Urbut et al., 2019). Mash was run in three stages following mash documentation (https://stephenslab.github.io/mash/r/articles/eQTL_outline.html): first, 10K SNPs were used as a 'random' set to learn the correlation structure among null tests; second, 1K SNPs with the maximum $-\log_{10}(p\text{-values})$ from the univariate GWAS were used to construct data-driven covariance matrices; third, the random set was used to fit the mashr model; fourth, posterior summaries using the model fit on the random set were computed on all 26K SNPs in the dataset. To allow mash to converge effectively on effect estimates, the effects for each phenotype were scaled, or standardized to fall between -1 and 1 with a mean of 0 . To assess when a SNP had evidence of a significant effect on a condition, we used local false sign rates (lfsr), which are analogous to false discovery rates but more conservative (in that they also reflect the uncertainty of the estimation of the sign of the effect) (Stephens, 2016). We used lfsr to find SNPs with \log_{10} -transformed Bayes factors > 2 in the mash model. Here, the Bayes factor is the ratio of the likelihood of one or more significant condition-specific SNP effects to the likelihood that the SNP had only null effects. We used a threshold of $\log_{10}BF$ (Bayes Factor) = 1.3 (equivalent to a FDR-adjusted p -value of 0.05). Code and data necessary to replicate this analysis are available at: <https://github.com/Alice-MacQueen/WAMIGXE>.

2.5. Candidate genes identification

We identified candidate genes corresponding to the significant SNPs

with effects higher than 0.1 (10% of the total trait variation for standardized effects) on at least two traits in all watering regimes. First, the flanking sequences corresponding to each of these SNPs (Wang et al., 2014) were used for BLAST searches using the wheat database URGI <http://urgi.versailles.inrae.fr/blast/aboutBlast.php> (Alaux et al., 2018), and the wheat IWGSC RefSeq v2.1 (Zhu et al., 2021). Next, we used the KnetMiner gene discovery platform (Hassani-Pak et al., 2021) <http://knetminer.org> to search for large genome-scale knowledge graphs and to visualize interesting subgraphs of connected information about the biology and functions of genes, gene networks, and traits. We did not map any significant SNPs associated with PH or GY that were mapped to the position of *Rht-B1b*, at the top of chromosome 4B, or *Rht-D1b*, at 70cM on chromosome 4D. Therefore, we analyzed the possible haplotypes using the 4 and 7 SNPs associated with these genes, respectively, at both positions using HAPLOTYPE ANALYSIS (Eliades and Eliades, 2009) to validate the effect of *Rht-B1b* or *Rht-D1b* on both traits.

3. Results

3.1. Population performance and statistical analysis

A total of 9 physiological and yield related traits were analyzed under three watering regimes. Broad sense heritability ranged from 0.48 to 0.97 , obtained for Chl and BY, respectively, measured in the well-watered treatment in the 2018–2019 growing season. Our results revealed substantial phenotypic variation for the measured traits within and between the three water regimes (Table 2). For example, the average plant heights were 91.5 and 90.7 cm under well-watered, 78.1 and 75.9 cm under mild stress, and 66.3 and 60.6 cm under severe stress conditions in 17/18 and 18/19 growing seasons, respectively. Average BY across all genotypes was reduced by 38.9 – 55.9% in the mild and severe drought treatments, respectively. Average GY across all genotypes was 16.35 g in well-watered conditions and reduced to 11.55 g in mild stress conditions and 8.19 g in severe stress conditions. Nine genotypes, 294568, 3597332, 346403, 1706327, 393392, 4314513, 4342318, 4885594, and 5535482, out-yielded the check cultivars in the well-watered conditions (Supplementary Table 2). Three genotypes, 4314513, 4342318, 4885594, out-yielded the check cultivars in the mild stress conditions. Three genotypes, 3597332, 4314513, 4342318, either out-yielded or were very close to the check cultivars in the severe stress conditions. Frequency distributions of some of the measured traits over the whole population showed transgression beyond both Egyptian check cultivars (Fig. 1) in the three watering regimes. Significant genotype by treatment (GxT) interactions were observed for all traits (Table 3).

Phenotypic correlation analysis (Fig. 2) showed significant positive correlations between the same trait when measured in the similar treatment in both growing seasons 17/18 and 18/19. Comparing the same watering regime in both growing seasons revealed significant positive correlations between GY, PH, SPKL, SPKN, TN, and BY. Harvest index showed a negative correlation with all traits, except for Chl and GY, under the three watering regimes. Negative correlations were observed between CT and both Chl and GY under the three watering regimes in both growing seasons.

3.2. Multivariate genome-wide association mapping

In total, 457 SNPs had significant effects on one or more measured

Table 2
 Estimation of the minimum (Min), maximum (Max), average (Avg), and heritability (H^2) of the studied traits under well-watered, mild stress, and severe stress conditions. Sa and Sha represent the two Egyptian check cultivars Sahel-1 and Shandweel-1, respectively. Chlorophyll content (Chl), Canopy temperature (CT), Plant height (PH) in centimeters (cm), number of tillers (TN), spike length (SPKL), number of spikes (SPKN), biological yield (BY), grain yield (GY) per plant, and harvest index (HI).

Season	Trait / units	Well-watered						Mild stress						Sever stress					
		Min	Max	Avg	H2	Sa	Sha	Min	Max	Avg	H2	Sa	Sha	Min	Max	Avg	H2	Sa	Sha
		2017	Chl	41.8	63.4	53.3	0.75	57.3	59.8	38.4	53.2	45.2	0.62	42.4	45.9	29.9	48.3	38.0	0.50
	CT (°C)	18.7	29.9	23.1	0.73	21.2	20.6	21.3	32.3	26.4	0.74	22.6	23.5	22.8	38.2	29.6	0.73	24.4	25.0
	PH (cm)	61.0	115.0	91.6	0.73	101.0	99.8	58.0	103.0	78.1	0.96	87.6	87.3	37.7	91.0	66.3	0.96	75.6	73.1
	SPKL (cm)	8.0	14.9	11.1	0.77	10.3	9.2	6.0	13.0	9.2	0.63	8.8	8.3	5.0	11.7	7.5	0.59	7.8	7.6
	SPKN	3.2	9.8	7.0	0.71	7.5	8.1	2.3	7.3	4.6	0.64	6.0	6.0	1.7	6.7	3.7	0.57	5.5	5.5
	TN	4.7	12.0	7.9	0.74	8.0	9.4	3.7	9.0	6.3	0.62	7.2	7.5	2.0	8.0	4.9	0.67	6.7	7.0
	BY (g)	41.8	127.7	76.5	0.92	81.1	87.9	28.9	76.6	47.0	0.82	53.9	56.9	18.6	52.7	33.7	0.74	41.7	45.2
	GY (g)	9.2	28.8	16.4	0.82	19.9	22.3	6.7	17.6	12.4	0.52	15.8	15.8	4.8	15.2	8.6	0.68	12.0	12.2
	HI	10.1	47.7	22.6	0.85	31.2	28.5	13.5	40.4	27.0	0.59	30.2	29.7	13.2	44.1	26.4	0.78	29.8	31.0
2018	Chl	37.5	72.1	53.2	0.48	59.7	60.3	28.3	66.9	39.8	0.57	46.8	47.8	20.1	42.2	30.8	0.70	38.3	38.8
	CT (°C)	18.2	29.4	23.0	0.63	23.3	23.2	20.2	33.3	26.2	0.67	24.2	22.8	22.7	46.2	30.6	0.58	26.6	26.9
	PH (cm)	38.6	115.5	90.8	0.92	103.2	101.3	50.5	101.8	75.9	0.91	89.7	87.9	38.7	90.7	60.6	0.93	77.3	72.5
	SPKL (cm)	7.0	14.2	10.8	0.57	10.9	9.4	4.8	11.2	8.2	0.69	9.1	8.5	3.9	10.2	6.6	0.75	7.6	7.5
	SPKN	3.7	12.8	6.8	0.81	7.9	8.0	2.8	7.5	5.0	0.58	6.1	6.2	1.7	5.7	3.4	0.58	5.5	5.7
	NT	4.3	12.9	7.8	0.84	8.9	8.8	3.4	9.7	5.9	0.67	7.5	8.3	2.3	7.7	4.7	0.69	7.0	6.7
	BY (g)	40.4	118.2	72.4	0.97	83.9	90.0	26.9	71.1	43.9	0.77	56.2	58.7	18.3	51.7	31.8	0.83	43.8	43.1
	GY (g)	6.1	30.3	16.2	0.90	22.0	24.0	5.7	19.3	10.6	0.85	16.1	16.4	3.7	10.7	7.7	0.86	12.4	12.6
	HI	10.7	47.3	23.4	0.91	33.8	30.1	12.9	38.0	24.9	0.78	32.0	31.3	13.6	39.7	25.0	0.80	32.0	29.6

trait (Fig. 3 and Supplementary Table 3) and had significant interactions with the water regimes and growing seasons. There were two major and two minor patterns of phenotypic effects in the data. First, 337 significant SNPs had the majority of their posterior weight in mash on the data-driven model ED_PCA_1. This pattern had positive pleiotropic effects on GY and its related traits, PH, SPKL, SPKN, TN, BY, and Chl; these SNPs typically had nonsignificant or significant negative effects on CT or HI. Second, 52 significant SNPs had significant conditionally neutral effects on Chl measured under only one water regime. In addition, 14 significant SNPs had effects on Chl measured under stressed conditions in 2017, and three significant SNPs ad effects on GY in control conditions in 2017, and otherwise were conditionally neutral. We mapped 61 SNPs with effects greater than 0.10 in at least one environment. For example, 2 SNPs, Ku_c18550_1388 and Kukri_c26718_319, located on chromosome 3D between 610.3 and 611.1 Mb were significant at $\log_{10}BF = 7.42$. The alternate allele of those 2 SNPs increased trait values for all traits under all water regimes, with the exception that antagonistic pleiotropic effects were observed for CT and HI. For these SNPs for CT, negative effects were observed under mild and severe stress in both growing seasons. In contrast, both SNPs showed negative effects on HI in all treatment-season combinations; these effects were strongest under severe stress. Similar effects were observed for 2 SNPs with $\log_{10}BF = 7.42$, D_GA8KES401DOK1W_269 and D_GDRF1KQ01 AX2L0_245, on chromosome 7D between 188382841 and 188383088, and 542677391–542677557 bp, respectively. The interval where both SNPs are located, 188.3 – 625.8 Mb, included an additional 6 significant SNPs with similar effects as above. On the other hand, some SNPs showed negative effects on the measured traits, including BS00045521_51, BobWhite_c14508_181, RAC875_rep_c89232_502, BS00024617_51, and BS00087197_51 on chromosomes 2A, 4A, 5D, 7A, and 7B, respectively. Those 5 SNPs decreased trait values for all traits under all water regimes, however, antagonistic pleiotropic effects were again observed for CT and HI. For CT, positive effects were observed under mild stress in both growing seasons and under severe stress in the 17/18 growing season. In contrast, SNP effects on HI were positive in all treatment-season combinations, except in the control treatment of the 17/18 growing season.

3.3. Candidate gene identification

We looked for candidate genes associated with the 61 significant SNPs with effects higher than 0.1 on at least two phenotypes in all environments. Our analysis revealed 46 candidate genes (Supplementary Table 4) of which eleven genes were previously reported to have direct effects on some of the measured traits. For example, the gene TraesCS4B02G009900 is reported to control quality traits and grain weight. The gene TraesCS7D03G1184700 was responsible for semi-dwarf growth habits. Another gene, TraesCS7A03G0883000, had effects on plant response to drought, plant height, and days to heading. On the other hand, haplotype analysis for the 4 SNPs located on the top of chromosome 4B between 0 and 1 cM (between 0.9 and 5.6 Mb) (Supplementary Tables 4 and 5), where *Rht-B1b* is located, and for the 7 SNPs at 70 cM (between 26.1 and 29.0 Mb) on chromosome 4D (Supplementary Tables 4 and 6), where *Rht-D1b* is located, revealed significant interaction between GY and both of watering regimes and growing seasons. For example, in case of *Rht-B1b*, we found significant differences in both growing seasons between the following haplotype groups; GCAA and GCGG in the mild stress regime, ACGG and GCAA in the control and mild stress regimes, and between ATAA and GCAA in the control regime. In addition, in case of *Rht-D1b*, our analysis showed significant differences between the two haplotype groups CACACCC and CAAACCC measured under mild and severe stresses but only in the second growing season 18/19.

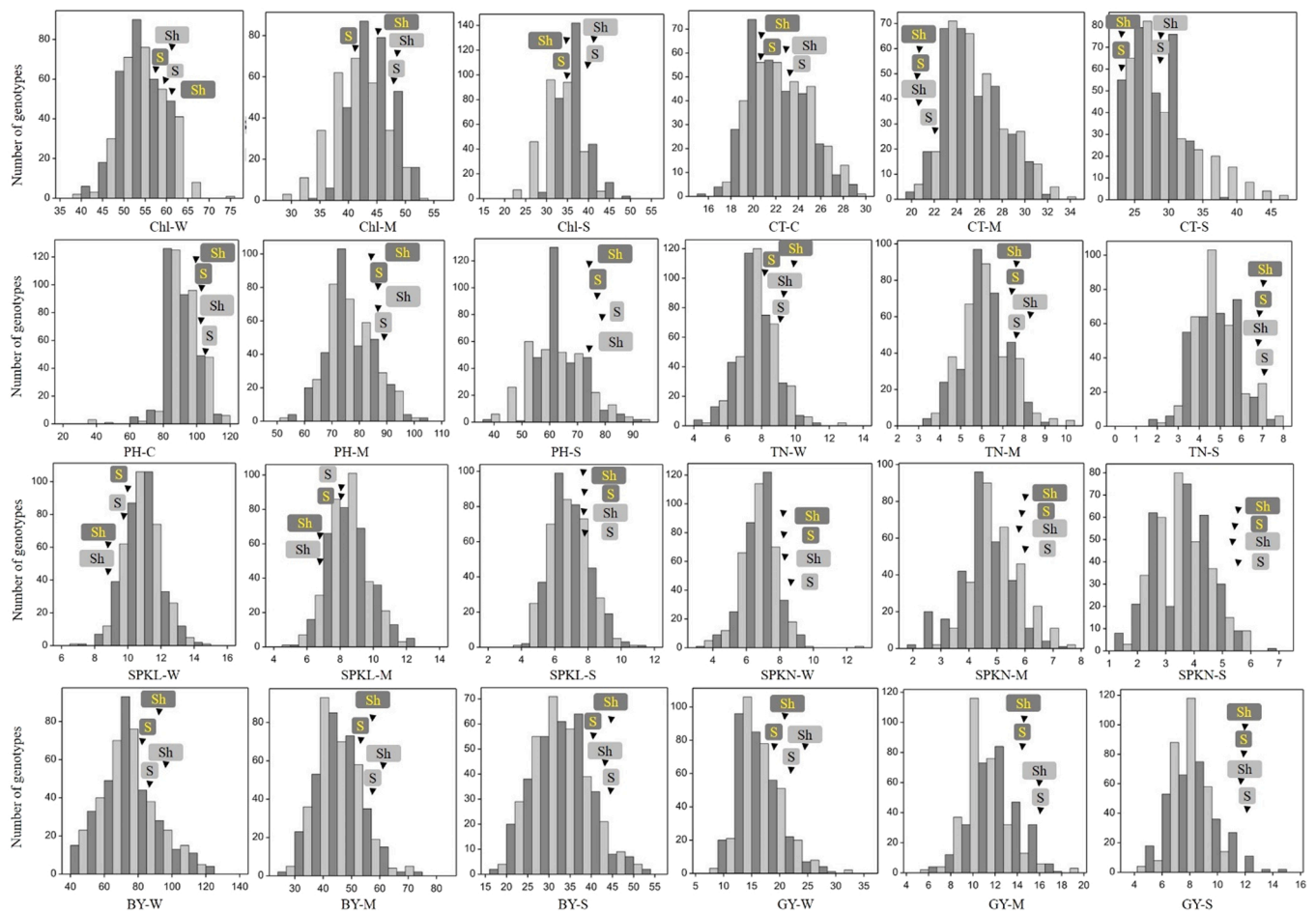


Fig. 1. Frequency distributions of the non-normalized trait values for the WAMI population grown under well-watered (W), mild stress (M), severe stress (S) regimes in two growing seasons 17/18 (dark gray), and 18/19 (light gray). Vertical axes indicate the number of lines per trait value class, and horizontal axes indicate the different trait value classes. The two Egyptian check cultivars are indicated as S for Sahil and Sh for Shandwel Trait abbreviations are given in Table 2.

Table 3

ANOVA table representing mean squares of the measured traits, Chlorophyll content (Chl), Canopy temperature (CT), Plant height (PH) in centimeters (cm), number of tillers (TN), spike length (SPKL), number of spikes (SPKN), biological yield (BY), grain yield (GY), and harvest index (HI). S.O.V = source of variation, DF = degree of freedom, Y = year, E = error, T = treatments, G = genotype, and x = the interaction between different S.O.V.

S.O.V.	D.F.	Chl	CT	PH	TN	SPKL	SPKN	BY	GY	HI
Y	1	24552.21**	77.93**	10047.43**	5940.07**	780.55**	12.38**	1088036.26**	47289.34**	1542.55**
E (a)	2	40.39	97.03	424.27	2.12	21.04	1.69	152.29	46.07	77.29
T	2	150571.76**	21518.61**	334025.17**	5531.03**	6890.02**	4908.47**	193650.42**	5554.18**	2265.01**
Y x T	2	5225.90**	191.94**4	3128.64**	212.30**	42.70**	59.34**5	63919.48**	842.62**	3242.21**
E (b)	4	167.9451	39.41	117.19	0.518	5.914	39.27	19.90	8.72	34.81
G	288	141.45**	90.22**	703.44**	8.40**	16.68**6	10.03**	910.34**	56.37**	267.76**
Y x G	288	43.15**	15.21**3	90.84**	6.10**	3.95**	0.919**	580.00**	26.63**	121.93**4
E (c)	576	16.95	4.73	9.92	0.491	2.56	0.531	17.63	2.38	11.49
T x G	576	51.64**	21.61**	273.11**	1.95**	4.71**	2.61**4	181.83**	10.34**	66.80**
Y x T x G	576	20.29**	9.32**	76.61**	1.50**	2.71**	0.538**	183.93**	7.45**	74.08**
E (d)	3456	10.62	3.07	7.19	0.422	1.24	0.244	13.97	1.51	8.34
C.V.%		8.92	7.7	3.96	9.22	16.96	11.92	7.49	10.16	11.95

4. Discussion

Wheat is the most widely grown crop on the planet, however, research investments in wheat lag behind those of other staple crops. It is expected that the global yield gains will not meet 2050 demands, and that climate stresses will further exacerbate this problem (Reynolds et al., 2021). This critical situation has an outsized impact on developing economies such as Egypt. Indeed, Egypt is one of the world’s leading wheat importers, importing 12 million tons/year, a figure that is expected to increase to over 15 million tons by 2028 (FAO, 2020). To

address this issue within Egypt, two parallel approaches have been taken: 1) cultivating wheat in new areas by reclaiming desert, which accounts for 96% of Egypt’s landscape and is subjected to abiotic stresses, such as drought (Abdelaal and Thilmany, 2019), and 2) selecting high yielding wheat varieties in current cultivation areas. Given that water scarcity hinders any plans to cultivate large reclaimed areas, breeding efforts should be directed toward selecting for high yielding, drought tolerant wheat varieties. Therefore, we aimed to select genotypes that perform better and yield higher than the two adapted local Egyptian check cultivars under both well-watered and drought

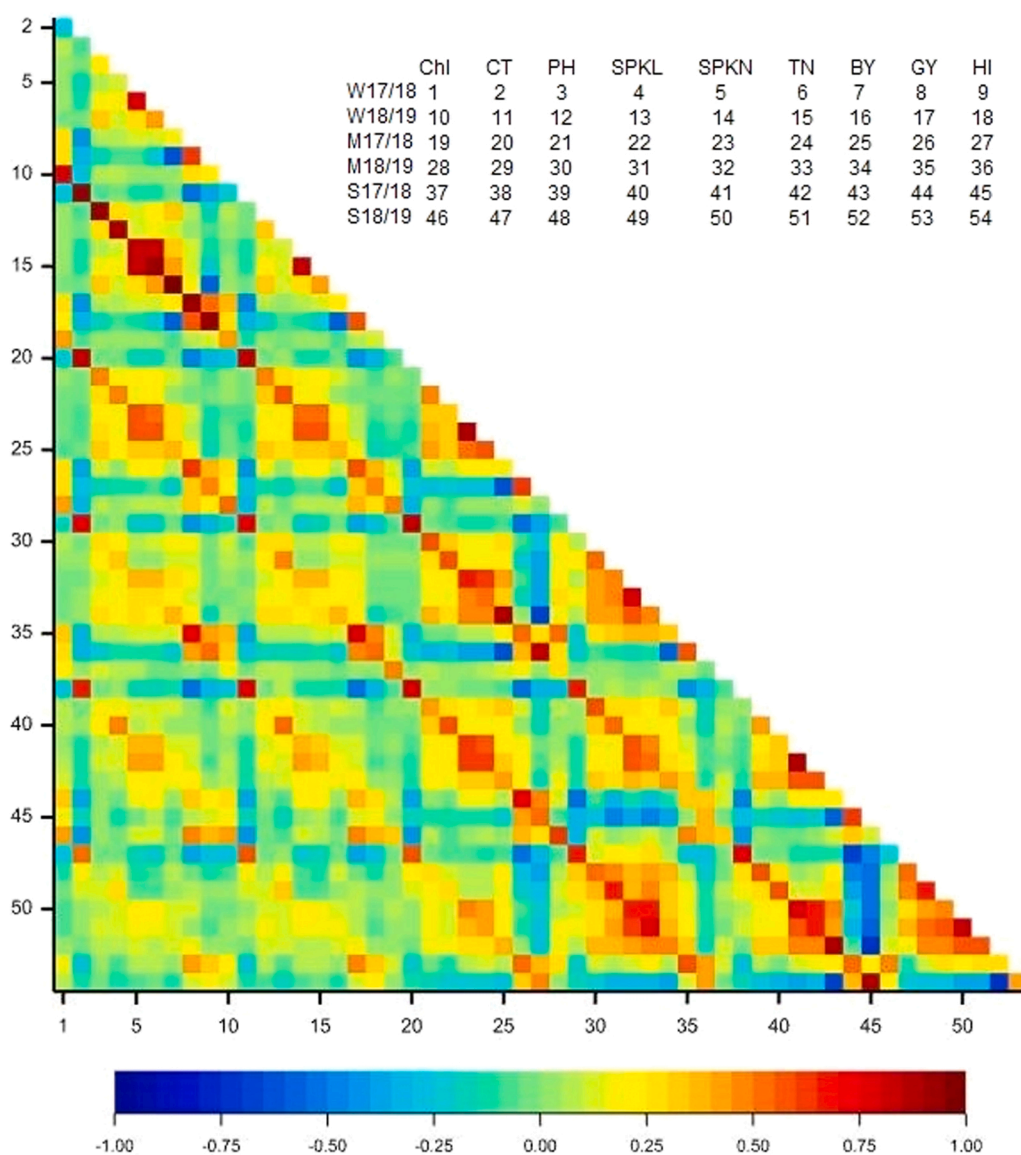


Fig. 2. Heat map showing the correlation between the measured traits under three watering regimes, well-watered (W), mild stress (M), and severe stress (S) in each growing season 17/18 and 18/19. Chlorophyll content (Chl), Canopy temperature (CT), Plant height (PH) in centimeters (cm), spike length (SPKL), number of spikes (SPKN), number of tillers (TN), biological yield (BY), grain yield (GY), and harvest index (HI). Each colored and numbered square represents a trait, and all combinations of traits, growing seasons, and treatments are explained in the key. A color scale showing the correlation values ranging from dark blue, -1 , to green, 0 , to 1 , dark red is shown below the heat map. (For interpretation of the references to colour in this figure legend, the reader is referred to the web version of this article.)

stress regimes. Our results revealed nine, three, and three genotypes that out-performed the GY of the two check cultivars under the control, mild and severe stress regimes, respectively. We observed G \times E for these genotypes, as six genotypes were selected under the well-watered regimes but failed to out-yield the two check cultivars under mild and severe stress regimes. The three stable genotypes can be further used for future crossing to provide information on the genetics controlling yield and its related traits or as parents in new breeding efforts. In addition, as the experimental site consists of newly reclaimed soil, we propose those high-yielding genotypes should be further evaluated and distributed in similar Egyptian reclaimed areas under drought stress conditions.

Upon screening the morphological and physiological performance of the 287 diverse advanced wheat lines, positive phenotypic correlations were observed between the same trait measured under the same water regime in both growing seasons, indicating reproducible results over growing seasons. We also observed significant positive correlations between GY and PH, TN, SPKL, SPKN, and BY under all water regimes highlighting their positive role in improving GY. This is a similar finding to the results of earlier studies under drought, heat, and combined stresses (Chen et al., 2012; Lopes et al., 2015; Mwadzingeni et al., 2016). However, we observed significant G \times E between the three watering regimes for all phenotypes. This G \times E was reflected in QTL \times E that was

detected using the 26814 SNPs (Ahirwar et al., 2018) and mash (Urbut et al., 2019). Mash enabled us to find SNPs that had similar or opposite effects on several traits in different water regimes, i.e. synergistic or antagonistic pleiotropic effects, respectively. Both effects are of great importance in breeding programs and should be carefully taken into account, because breeding for one trait might negatively affect other traits (Des Marais et al., 2013; El-Soda et al., 2014). For example, our analysis revealed two major QTLs on chromosomes 5D and 7D, spanning four SNPs in each of the intervals between 549.6 and 569.2 Mb and 193.4 and 476.0 Mb, respectively. Both QTLs affected all traits positively, except for CT under mild and severe stress regimes and HI under all treatments, where effects were antagonistically pleiotropic. Therefore, both QTLs are favorable in breeding programs as they increase GY and its related components, in addition, they keep CT as low as possible under stress regimes, an adaptive strategy to cope with drought (Lopes et al., 2013). Similar major effects were observed for the marker mapped on chromosome 7B between 213497302 and 213497384 bp. In contrast, non-favorable effects were observed for the QTL spanning 3 markers on chromosome 7B between 137.4 and 139.2 Mb with negative effects on all traits, and no effects on CT and HI in mild and severe stresses. We also detected conditional neutrality, where a QTL shows an effect on one trait in one environment but no effects in other environments. We observed

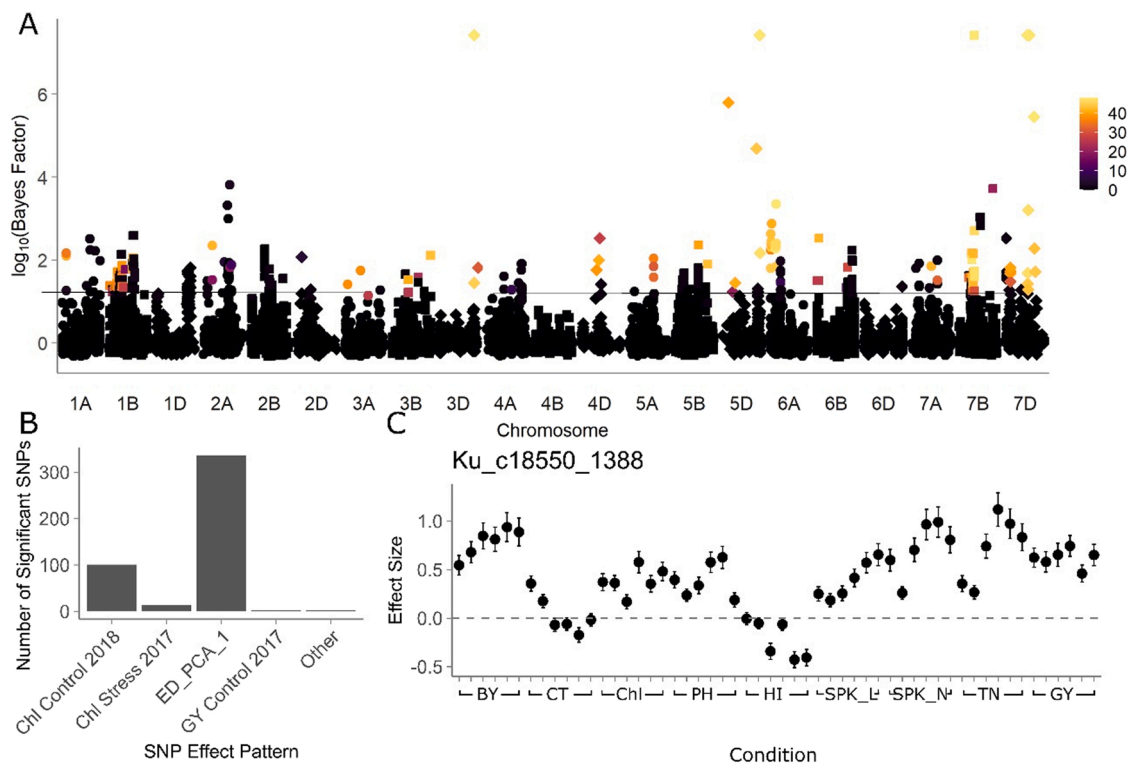


Fig. 3. Results of genome wide association mapping. A) Manhattan plot showing significant SNPs at Bayes factor \log_{10} ($\log_{10}BF$) of 1.3, presented by a horizontal line, (equivalent to a FDR-adjusted p -value of 0.05), associated with the measured traits. Point color represents the number of phenotypes for which the SNP has a local false-sign rate < 0.05 , or a significant effect on that phenotype. Circles represent the A subgenome, Squares represent the B subgenome, and diamonds represent the D subgenome. B) Barplot showing majority of posterior weight in mash model for particular patterns of SNP effects for the significant SNPs. ED_PCA_1 is a data-driven model generated by mash. C) SNP effects on all combinations of phenotype, treatment, and year for the most significant SNP in mash. This pattern of SNP effects corresponds to the ED_PCA_1 data-driven pattern of SNP effects generated by mash.

several QTLs with minor conditionally neutral effects that were mainly associated with Chl. For example, 11 SNPs distributed over chromosome 1A showed negative effects on Chl in the well-watered regime of the growing season 18/19.

Several SNPs mapped here were reported in earlier studies to be associated with the same or related traits under similar stresses. For example, *w SNP*_BF291549B_Ta_1_1, mapped on 1B, decreased PH under drought stress (Lopes et al., 2015) which is similar to our observation with negative effects not only on PH but also on Chl, TN, SPKL, SPKN, BY, and GY under all watering regimes. The same authors mapped another SNP, *w SNP*_Ex_c621_1230852, with a negative effect on heading dates (HD) under heat stress. We found negative effects of this SNP on GY in all water regimes, on SPKL under severe, and on SPKN and TN under moderate and severe stresses. Preferably, HD and GY correlate negatively thus we would expect this SNP to have a positive effect on GY, however, its negative effect on GY here would not be favorable in breeding programs. Another study that used the same 90K SNP array in a winter wheat population (Schulthess et al., 2017) found associations between Ra_c18630_284 and both GY and HD and between RAC875_c42715_856 and both GY and thousand-grain weight. We found that Ra_c18630_284 had significant effects on the yield components traits SPKN, TN, and BY under severe stress. RAC875_c42715_856 had significant effects on all traits. A recent study mapped a QTL for GY on chromosome 7B at 72.74 cM (Muhu-Din Ahmed et al., 2020); here, we mapped a SNP marker, CAP7_c1748_201, at this position, between 414036071 and 414036171 bp, with significant effects on all traits.

Plant height affects plant architecture, lodging resistance, and yield, and is one of the most significant agronomic variables in production (Allan, 1989; Wang et al., 2017). Twenty-two dwarfing genes or reduced height (*Rht*) genes were discovered in hexaploid wheat (Chai et al., 2021). Of these, *Rht-B1a* and *Rht-D1a* are wild-type alleles that encode

DELLA proteins, that have previously been proposed to be involved in plant acclimation responses to some stress conditions (Harberd et al., 2009). The introduction of the reduced stature semi-dwarfing genes, *Rht-B1b* and *Rht-D1b*, showed pleiotropic effects that significantly increased wheat GY (Hedden, 2003; Van De Velde et al., 2017; Gao et al., 2020), and reduced photosynthetic rates, evapotranspiration, and stomatal conductance (Jobson et al., 2019). *Rht-B1b* and *Rht-D1b* are on chromosomes 4B and 4D, respectively (Ellis et al., 2002), and similar to our results, both were not associated with PH when the WAMI population was evaluated under well-watered or drought regimes (Edae et al., 2014). *Rht-B1b* is located on the top of chromosome 4B (Lopes et al., 2015; Chai et al., 2021). However, we did not map any significant SNPs at this position, which could be due to the low minor allele frequency of SNPs at this candidate in the WAMI. Therefore, we performed a secondary haplotype analyses using the 4 SNPs located between 0.9 and 5.6 Mb on 4B. We found significant differences between two haplotype groups in each of the control, control and mild stress, and mild stress regimes. This result indicates that the role of *Rht-B1b* in controlling GY under drought stress is different from its role under the well-watered condition which is similar to an earlier observation (Jatayev et al., 2020). This observed GxE effect of the *Rht-B1b* was similar to the earlier report (Lopes et al., 2015) where *Rht-B1b* was responsible for the major $G \times E$ interaction for GY in the four different environments where the WAMI was tested. *Rht-D1b* was mapped to *w SNP*_Ex_rep_c107564_91144523 (Lopes et al., 2015), which is located at 70 cM, 27084935 – 27085135 bp, (Ahirwar et al., 2018), and was associated with PH under drought stress (Lopes et al., 2015), contradicting our results as none of the 7 SNPs in the interval between 26.1 and 29.0 Mb were associated with PH. The haplotype analysis of these SNPs revealed significant interaction with the growing seasons and watering regimes where GY was significantly different between two haplotype groups only

under mild and severe stresses in the second season 18/19.

We used gene annotation analysis of the sequences flanking the significant markers to propose candidate genes that might underlie GY and its related traits responses to drought stress. No genes were mapped to the position of the SNP D_F5XZDLF01CSICV_77. Therefore, we annotated the flanking sequences of the other 6 SNPs located between 26.1 and 29.0 Mb and found that wsnp_Ex_rep_c107564_91144523 was mapped in TraesCS4D03G0092300, a UDP-glucose 6-dehydrogenase, which was reported to enhance Arabidopsis growth and cold tolerance (Li et al., 2017). As none of the genes associated with the 6 SNPs had a direct effect on PH or GY, it could be that other genes in linkage disequilibrium are affecting those traits. Additional gene annotation analysis showed that the SNP Tdurum_contig31496_79 mapped to the gene TraesCS7B02G116000, ALUMINUM ACTIVATED MALATE TRANSPORTER4 (*ALMT4*) which was reported to be involved in the Arabidopsis stomatal closure in response to drought (Eisenach et al., 2017). Another SNP wsnp_Ex_c14622_22670594 was mapped to TraesCS3A02G143300, also known as ARABIDOPSIS TRITHORAX4 (*ATX4*). and its loss-of-function mutants in Arabidopsis showed drought stress-tolerant (Liu et al., 2018). The effects of both SNPs reduce GY and its components and increase CT under drought stress, two traits that are not favorable in breeding programs. In contrast, we mapped a significant SNP with $\log_{10}BF = 7.4$ in TraesCS3D03G1167800 (*E3* ubiquitin transferase or *PUB12*) with favorable positive and large effects on GY and its related traits, and negative effects on CT under stress treatments. The Arabidopsis *pub12*, *pub13*, and *pub12 pub13* mutants lost more water and were more sensitive to drought stress than the wild type plants (Lim et al., 2017).

5. Conclusion

We screened the WAMI population for 9 GY related traits with moderate to high heritability, indicating great potential for selection and GY improvements under the three examined watering regimes in Egypt. For example, we selected four genotypes with high GY that outperformed the two local check cultivars. Those six genotypes could be further evaluated all over the Egyptian governorates to select the highest yielding genotype in each governorate. In addition, they could be used to create a multi-parent population to further unravel the genetic factors underlying yield component traits. In addition, the data presented here can be further used for genomic selection and modeling wheat response to different watering regimes. The mapped main effect SNPs are good candidates to be used in marker assisted breeding programs that aim to improve wheat GY under non-stressed as well as drought conditions. The candidate genes identified here using the recently updated IWGSC RefSeq v2.1 need to be further validated as the genes underlying the observed phenotypic variation.

CCRediT authorship contribution statement

Alaa A Said: Investigation, Data analysis. **Alice H MacQueen:** Data analysis, Writing – review & editing. **Haitham Shawky:** Investigation. **Matthew Reynolds:** Resources, Reviewing manuscript. **Thomas E. Juenger:** Consulting, Reviewing manuscript. **Mohamed El-Soda:** Planning, Acquiring fund, Data analysis, Writing – original draft, Reviewing manuscript. All authors have read and agreed to the published version of the manuscript.

Declaration of Competing Interest

The authors declare that they have no known competing financial interests or personal relationships that could have appeared to influence the work reported in this paper.

Data Availability

All data supporting the findings of this study are available within the paper and within its [Supplementary materials](#) published online.

Acknowledgment

This paper is based upon work supported by Science, Technology & Innovation Funding Authority (STDF) under Grant number 25959.

Author contribution

Alaa A Said: performed the experiments; phenotyping; data analysis. Alice H MacQueen: data analysis; writing; reviewing manuscript. Haitham Shawky: phenotyping. Matthew Reynolds: resources; reviewing manuscript. Thomas E. Juenger: consulting; reviewing manuscript. Mohamed El-Soda: planning; acquiring fund; data analysis; writing; reviewing manuscript. All authors have read and agreed to the published version of the manuscript.

Appendix A. Supporting information

Supplementary data associated with this article can be found in the online version at [doi:10.1016/j.envexpbot.2021.104740](https://doi.org/10.1016/j.envexpbot.2021.104740).

References

- Abdelaal, H.S.A., Thilmann, D., 2019. Grains production prospects and long run food security in Egypt. *Sustainability* 11, 4457.
- Ahirwar, R.N., Mishra, V.K., Chand, R., Budhlakoti, N., Mishra, D.C., Kumar, S., Singh, S., Joshi, A.K., 2018. Genome-wide association mapping of spot blotch resistance in wheat association mapping initiative (WAMI) panel of spring wheat (*Triticum aestivum* L.). *PLoS One* 13, e0208196.
- Alaux, M., Rogers, J., Letellier, T., Flores, R., Alfama, F., Pommier, C., Mohellibi, N., Durand, S., Kimmel, E., Michotey, C., et al., 2018. Linking the international wheat genome sequencing consortium bread wheat reference genome sequence to wheat genetic and phenomic data. *Genome Biol.* 19, 111.
- Alexandratos, N., Bruinsma, J., 2012. World Agriculture Towards 2030/2050: The 2012 Revision. Food and Agriculture Organization of the United Nations, Rome (ESA Working Paper No. 12-03).
- Allan, R.E., 1989. Agronomic comparisons between Rht1 and Rht2 semidwarf genes in winter wheat. *Crop Sci.* 29.
- Allen, R., Pereira, L., Raes, D., Smith, M., 1998. Crop Evapotranspiration-Guidelines for Computing Crop Water Requirements-FAO Irrigation and Drainage Paper 56. Food and Agriculture Organization.
- Alqudah, A.M., Sallam, A., Stephen Baenziger, P., Börner, A., 2020. GWAS: fast-forwarding gene identification and characterization in temperate cereals: lessons from Barley – a review. *J. Adv. Res.* 22, 119–135.
- Chai, S., Yao, Q., Zhang, X., Xiao, X., Fan, X., Zeng, J., Sha, L., Kang, H., Zhang, H., Li, J., et al., 2021. The semi-dwarfing gene Rht-dp from dwarf polish wheat (*Triticum polonicum* L.) is the "Green Revolution" gene Rht-B1b. *BMC Genom.* 22, 63.
- Chen, X., Min, D., Yasir, T.A., Hu, Y.-G., 2012. Evaluation of 14 morphological, yield-related and physiological traits as indicators of drought tolerance in Chinese winter bread wheat revealed by analysis of the membership function value of drought tolerance (MFVD). *Field Crops Res.* 137, 195–201.
- Des Marais, D.L., Hernandez, K.M., Juenger, T.E., 2013. Genotype-by-environment interaction and plasticity: exploring genomic responses of plants to the abiotic environment. *Annu. Rev. Ecol. Syst.* 44, 5–29.
- Eadae, E.A., Byrne, P.F., Haley, S.D., Lopes, M.S., Reynolds, M.P., 2014. Genome-wide association mapping of yield and yield components of spring wheat under contrasting moisture regimes. *Theor. Appl. Genet.* 127, 791–807.
- Eisenach, C., Baetz, U., Huck, N.V., Zhang, J., De Angeli, A., Beckers, G.J.M., Martinoia, E., 2017. ABA-induced stomatal closure involves ALMT4, a phosphorylation-dependent vacuolar anion channel of arabidopsis. *Plant Cell* 29, 2552–2569.
- El-Soda, M., Malosetti, M., Zwaan, B.J., Koornneef, M., Aarts, M.G., 2014. Genotype x environment interaction QTL mapping in plants: lessons from Arabidopsis. *Trends Plant Sci.* 9, 390–398.
- El-Soda, M., Sarhan, S.M., 2021. From gene mapping to gene editing, a guide from the Arabidopsis research. *Annu. Plant Rev. Online* 4, 1–32.
- Eliades, N.-G., Eliades, D.G. 2009. HAPLOTYPE ANALYSIS: software for analysis of haplotypes data. Distributed by the authors. Forest Genetics and Forest Tree Breeding, Georg-August University Goettingen, Germany.
- Ellis, M., Spielmeier, W., Gale, K., Rebetzke, G., Richards, R., 2002. "Perfect" markers for the Rht-B1b and Rht-D1b dwarfing genes in wheat. *Theor. Appl. Genet.* 105, 1038–1042.
- Falconer, D.S., 1952. The problem of environment and selection. *Am. Nat.* 86, 293–298.

- Gao, Z., Wang, Y., Tian, G., Zhao, Y., Li, C., Cao, Q., Han, R., Shi, Z., He, M., 2020. Plant height and its relationship with yield in wheat under different irrigation regime. *Irrig. Sci.* 38, 365–371.
- Harberd, N.P., Belfield, E., Yasumura, Y., 2009. The angiosperm gibberellin-GID1-DELLA growth regulatory mechanism: how an “Inhibitor of an Inhibitor” enables flexible response to fluctuating environments. *Plant Cell* 21, 1328–1339.
- Hassani-Pak, K., Singh, A., Brandizi, M., Hearnshaw, J., Parsons, J.D., Amberkar, S., Phillips, A.L., Doonan, J.H., Rawlings, C., 2021. KnetMiner: a comprehensive approach for supporting evidence-based gene discovery and complex trait analysis across species. *Plant Biotechnol. J.*
- Hedden, P., 2003. The genes of the green revolution. *Trends Genet.* 19, 5–9.
- Jatayev, S., Sukhikh, I., Vavilova, V., Smolenskaya, S.E., Goncharov, N.P., Kurishbayev, A., Zotova, L., Absattarova, A., Serikbay, D., Hu, Y.-G., et al., 2020. Green revolution ‘stumbles’ in a dry environment: dwarf wheat with Rht genes fails to produce higher grain yield than taller plants under drought. *Plant Cell Environ.* 43, 2355–2364.
- Jobson, E.M., Johnston, R.E., Oiestad, A.J., Martin, J.M., Giroux, M.J., 2019. The impact of the wheat Rht-B1b semi-dwarfing allele on photosynthesis and seed development under field conditions. *Front. Plant Sci.* 10.
- Li, N.N., Chen, L., Li, X.H., Li, Q., Zhang, W.B., Takechi, K., Takano, H., Lin, X.F., 2017. Overexpression of UDP-glucose dehydrogenase from *Larix gmelinii* enhances growth and cold tolerance in transgenic *Arabidopsis thaliana*. *Biol. Plant.* 61, 95–105.
- Lim, C.W., Park, C., Kim, J.-H., Joo, H., Hong, E., Lee, S.C., 2017. Pepper CaREL1, a ubiquitin E3 ligase, regulates drought tolerance via the ABA-signalling pathway. *Sci. Rep.* 7, 477.
- Liu, Y., Zhang, A., Yin, H., Meng, Q., Yu, X., Huang, S., Wang, J., Ahmad, R., Liu, B., Xu, Z.-Y., 2018. Trithorax-group proteins ARABIDOPSIS TRITHORAX4 (ATX4) and ATX5 function in abscisic acid and dehydration stress responses. *New Phytol.* 217, 1582–1597.
- Lopes, M.S., Dreisigacker, S., Pena, R.J., Sukumaran, S., Reynolds, M.P., 2015. Genetic characterization of the wheat association mapping initiative (WAMI) panel for dissection of complex traits in spring wheat. *Theor. Appl. Genet.* 128, 453–464.
- Lopes, M.S., Reynolds, M.P., McIntyre, C.L., Mathews, K.L., Jalal Kamali, M.R., Mossad, M., Feltaous, Y., Tahir, I.S.A., Chatrath, R., Ogbonnaya, F., et al., 2013. QTL for yield and associated traits in the Seri/Babax population grown across several environments in Mexico, in the West Asia, North Africa, and South Asia regions. *Theor. Appl. Genet.* 126, 971–984.
- MacQueen, A.H., Zhang, L., Bonnette, J., Boe, A.R., Fay, P.A., Fritschi, F.B., Lowry, D.B., Mitchell, R.B., Rouquette, F.M., Wu, Y., et al., 2021. Mapping of genotype-by-environment interactions in phenology identifies two cues for flowering in switchgrass (*Panicum virgatum*). *bioRxiv* (456975), 2021.2008.2019.
- Manès, Y., Gomez, H.F., Puhl, L., Reynolds, M., Braun, H.J., Trethowan, R., 2012. Genetic yield gains of the CIMMYT international semi-arid wheat yield trials from 1994 to 2010. *Crop Sci.* 52, 1543–1552.
- Mathew, I., Shimelis, H., Shayanowako, A.I.T., Laing, M., Chaplot, V., 2019. Genome-wide association study of drought tolerance and biomass allocation in wheat. *PLoS One* 14, e0225383.
- Muhu-Din Ahmed, H.G., Sajjad, M., Zeng, Y., Iqbal, M., Habibullah Khan, S., Ullah, A., Nadeem, Akhtar, M., 2020. Genome-wide association mapping through 90K SNP array for quality and yield attributes in bread wheat against water-deficit conditions. *Agriculture* 10, 392.
- Mwadingeni, L., Shimelis, H., Tesfay, S., Tsilo, T.J., 2016. Screening of bread wheat genotypes for drought tolerance using phenotypic and proline analyses. *Front. Plant Sci.* 7.
- Pinto, R.S., Reynolds, M.P., Mathews, K.L., McIntyre, C.L., Olivares-Villegas, J.-J., Chapman, S.C., 2010. Heat and drought adaptive QTL in a wheat population designed to minimize confounding agronomic effects. *Theor. Appl. Genet.* 121, 1001–1021.
- Privé, F., Aschard, H., Ziyatdinov, A., Blum, M.G.B., 2018. Efficient analysis of large-scale genome-wide data with two R packages: bigstatsr and bigsnpr. *Bioinformatics* 34, 2781–2787.
- Privé, F., Luu, K., Blum, M.G.B., McGrath, J.J., Vilhjálmsson, B.J., 2020. Efficient toolkit implementing best practices for principal component analysis of population genetic data. *Bioinformatics* 36, 4449–4457.
- Reynolds, M.P., Lewis, J.M., Ammar, K., Basset, B.R., Crespo-Herrera, L., Crossa, J., Dhugga, K.S., Dreisigacker, S., Juliana, P., Karwat, H., et al., 2021. Harnessing translational research in wheat for climate resilience. *J. Exp. Bot.*
- Schulthess, A.W., Reif, J.C., Ling, J., Plieske, J., Kollers, S., Ebmeyer, E., Korzun, V., Argillier, O., Stiewe, G., Ganal, M.W., et al., 2017. The roles of pleiotropy and close linkage as revealed by association mapping of yield and correlated traits of wheat (*Triticum aestivum* L.). *J. Exp. Bot.* 68, 4089–4101.
- Shahinnia, F., Le Roy, J., Laborde, B., Sznajder, B., Kalambettu, P., Mahjourimajd, S., Tilbrook, J., Fleury, D., 2016. Genetic association of stomatal traits and yield in wheat grown in low rainfall environments. *BMC Plant Biol.* 16, 150.
- Sid'ko, A.F., Botvich, I.Y., Pisman, T.I., Shevyrnogov, A.P., 2017. Estimation of chlorophyll content and yield of wheat crops from reflectance spectra obtained by ground-based remote measurements. *Field Crops Res.* 207, 24–29.
- Stephens, M., 2016. False discovery rates: a new deal. *Biostatistics* 18, 275–294.
- Urbut, S.M., Wang, G., Carbonetto, P., Stephens, M., 2019. Flexible statistical methods for estimating and testing effects in genomic studies with multiple conditions. *Nat. Genet.* 51, 187–195.
- Van De Velde, K., Chandler, P.M., Van Der Straeten, D., Rohde, A., 2017. Differential coupling of gibberellin responses by Rht-B1c suppressor alleles and Rht-B1b in wheat highlights a unique role for the DELLA N-terminus in dormancy. *J. Exp. Bot.* 68, 443–455.
- Wang, S., Wong, D., Forrest, K., Allen, A., Chao, S., Huang, B.E., Maccaferri, M., Salvi, S., Milner, S.G., Cattivelli, L., et al., 2014. Characterization of polyploid wheat genomic diversity using a high-density 90 000 single nucleotide polymorphism array. *Plant Biotechnol. J.* 12, 787–796.
- Wang, Y., Zhao, J., Lu, W., Deng, D., 2017. Gibberellin in plant height control: old player, new story. *Plant Cell Rep.* 36, 391–398.
- Zhu, T., Wang, L., Rimbart, H., Rodriguez, J.C., Deal, K.R., De Oliveira, R., Choulet, F., Keeble-Gagnère, G., Tibbits, J., Rogers, J., et al., 2021. Optical maps refine the bread wheat *Triticum aestivum* cv. Chinese Spring genome assembly. *Plant J.* 107, 303–314.